The Journal of Chemical Physics

RESEARCH ARTICLE | OCTOBER 23 2025

Solvent-mediated mechanism and kinetics of glucose mutarotation from enhanced sampling simulations

Special Collection: Michele Parrinello Festschrift

Francesco Serse ; Silvio Trespi; Matteo Paloni ; Matteo Salvalaglio ; Marco Mazzotti

J. Chem. Phys. 163, 164504 (2025)
https://doi.org/10.1063/5.0288357

The Journal of Chemical Physics ARTICLE pubs.aip.org/aip/jcp

Solvent-mediated mechanism and kinetics of glucose mutarotation from enhanced sampling simulations

Cite as: J. Chem. Phys. 163, 164504 (2025); doi: 10.1063/5.0288357
Submitted: 30 June 2025 • Accepted: 5 October 2025 •
Published Online: 23 October 2025

Francesco Serse,[1] Silvio Trespi,[2] Matteo Paloni,[3] Matteo Salvalaglio,[3,a)] and Marco Mazzotti[2,b)]

AFFILIATIONS

[1] Department of Chemistry, Materials and Chemical Engineering, Politecnico di Milano, Milan, Italy
[2] Institute of Energy and Process Engineering, ETH Zurich, 8092 Zurich, Switzerland
[3] Thomas Young Centre and Department of Chemical Engineering, University College London, London WC1E 7JE, United Kingdom

Note: This paper is part of the JCP Special Topic, Michele Parrinello Festschrift.
[a)] **Author to whom correspondence should be addressed:** m.salvalaglio@ucl.ac.uk
[b)] marco.mazzotti@ipe.mavt.ethz.ch

ABSTRACT

Understanding how solvent molecules participate in chemical reaction mechanisms remains a central challenge in molecular simulations. Here, we investigate the mechanism and kinetics of glucose mutarotation in aqueous solution using a combined well-tempered metadynamics and mean force integration approach, within the framework of canonical transition state theory. We compute free energy landscapes and kinetic rate coefficients for the $\alpha \rightarrow \beta$ mutarotation in pure water, as well as in systems representative of water/methanol and water/acetone mixtures. Our simulations indicate that ring opening and closure occur via concerted, solvent-assisted pathways, with ring opening identified as the rate-determining step. The temperature dependence of the predicted kinetic constant is quantitatively consistent with experimental data, while the reactivity modulation by organic co-solvents is captured qualitatively. Overall, the results provide molecular-level insight into solvent-mediated carbohydrate chemistry, demonstrating that the solvent participates in all key reactive steps and highlighting how enhanced sampling techniques can yield mechanistic and kinetic information in explicitly solvated reactive systems.

I. INTRODUCTION

Mutarotation in aqueous solutions is a key conformational transformation in carbohydrate chemistry, relevant to both fundamental understanding of isomerization in solution[1–4] and practical applications in fields such as pharmaceuticals and food science.[5–7] In this work, we investigate glucose as a representative monosaccharide for a broader class of carbohydrates that exhibit mutarotation, mediating the conformational transformation between two pyranose isomers in solution (see Fig. 1). By focusing on glucose, whose mutarotation centers on the same glucose moiety present in lactose and other disaccharides, we aim to reveal molecular-level features that underpin mutarotation across a broader range of carbohydrates.

Two mechanistic pathways have been proposed for this interconversion: one involving an acyclic intermediate formed via ring opening and another proceeding through a transient cyclic oxocarbenium ion. Under neutral aqueous conditions, experimental evidence supports the acyclic mechanism. Yet, several mechanistic aspects remain unresolved, particularly the degree of concertedness in the elementary steps, the catalytic role and number of participating solvent molecules, and the sensitivity of activation barriers to the solvent environment.

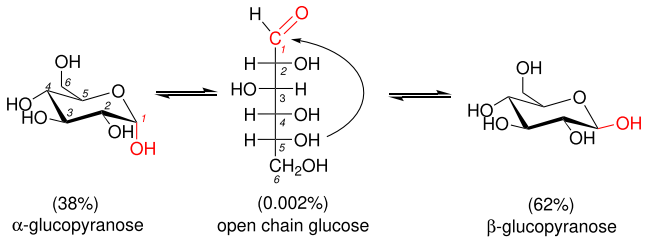

FIG. 1. Equilibrium between pyranoses and the open chain isomers of glucose. The relative amounts are from Angyal.[8] α- and β-glucopyranoses differ in the orientation of the hydroxyl group at C_1 (highlighted in red): axial or equatorial, respectively.

D-Glucose, the most abundant aldohexose sugar, also known as dextrose, exists in aqueous solution as a dynamic equilibrium mixture of structural isomers, as shown in Fig. 1. Indeed, the electrophilic carbonyl group of the linear open-chain form can undergo an intramolecular nucleophilic attack by one of the hydroxyl groups, leading to the formation of cyclic hemiacetals. If the hydroxyl group attached to the fourth carbon of the chain, C_4, has reacted to form a five-membered ring, the cyclic isomer is termed glucofuranose. Conversely, if the hydroxyl group of the C_5 has reacted, the six-membered ring is termed glucopyranose. In both cases, the cyclization generates a new chiral center at the carbon C_1, giving rise to α and β diastereomers, depending on the orientation of the hydroxyl group. The diastereomers are usually called anomers, and C_1 is called the "anomeric carbon."

In solution, equilibrium is established between the linear and cyclic forms, and the corresponding reaction network is called mutarotation. The equilibrium composition is specific to each compound and dependent on the solvent and the temperature, as shown in Table I. For the case of glucose dissolved in deuterium oxide at 31 °C, Angyal[8] reports that the pyranose isomers account for almost all the glucose present in solution. The furanoses and the open-chain account for less than 0.2% and 0.002%, respectively. When only two isomers are in appreciable amounts, the system exhibits simple mutarotation, as seen with glucose and xylose in water.[10] Other sugars, such as arabinose, fructose, ribose, or talose, have a significant concentration of both furanoses and pyranoses in solution and are said to exhibit complex mutarotation.[10]

Two mechanisms have been proposed to describe pyranose interconversion in aqueous solution, illustrated schematically in Fig. 2.[11] The first, known as the acyclic intermediate mechanism or Pedersen mechanism,[12] starts with the opening of the ring, yielding the open chain intermediate, which undergoes ring closure with inversion of configuration at the C_1. The ring opening determines the rate of mutarotation. It involves three elementary steps: (1) deprotonation of the hydroxyl group at C_1, (2) protonation of the ring oxygen O_5, and (3) cleavage of the C_1–O_5 bond to yield the open chain form. Water serves as both the solvent and the amphoteric catalyst, acting as both a Brønsted acid and a base. The second mechanism, known as the cyclic intermediate mechanism, starts with the protonation of the hydroxyl group at C_1, followed by its release as a water molecule and the formation of a cyclic oxocarbenium ion intermediate. The nucleophilic attack of a solvent water molecule on the carbocation results in inversion of configuration and regeneration of the proton catalyst.

Experimental evidence supports the acyclic intermediate mechanism under mildly acidic and neutral conditions in water (pH 2.5–7), where the rate of glucose mutarotation remains nearly constant.[13] Notably, it has been observed[14–16] that glucose labeled at the anomeric oxygen with ^{18}O undergoes oxygen exchange with the solvent at a rate significantly smaller than the measured rate of mutarotation. This rules out the cyclic intermediate mechanism because oxygen exchange with water is part of the reaction network. The timing of the three elementary steps that lead to ring opening remains a subject of active discussion: according to the analysis of isotope effects by Lewis *et al.*,[17] the deprotonation of O_1 precedes the protonation of the O_5 and the C_1–O_5 bond cleavage. Another research question is the number of water molecules involved in the catalysis. Alkorta and Popelier[18] computationally investigated the furanose interconversion of erythrose and treose at the B3LYP/6-311++G(d,p) level, explicitly including water molecules. They highlight the high mutarotation energy barrier of the isolated carbohydrate in the absence of water and its substantial reduction by inclusion of at least one water molecule. Plazinski *et al.*[19] elucidated the mechanism of ring-opening of glucose at the BP86/6-31+G(d) level, including eight water molecules and explicitly describing the remaining solvent molecules using a QM/MM approach. They observed catalytic pathways directly involving one or two water molecules in the proton transfer; however, the results indicate that catalysis by one water molecule is more probable. Indeed, the role of solvent molecules in modulating

TABLE I. Percent equilibrium composition of sugars in solution.

Sugar	Solvent	Temperature (°C)	Furanose		Pyranose		Open chain	Source
			α	β	α	β		
Glucose	D_2O	31	0	0.14	38	62	0.002	Angyal[8]
Xylose	D_2O	31	0.5		36.5	63	0.02	Angyal[8]
Ribose	D_2O	31	6.5	13.5	21.5	58.5	0.05	Angyal[8]
Talose	D_2O	22	16	13	42	29	0.03	Angyal[8]
Arabinose	D_2O	31	2.5	2	60	35.5	0.03	Angyal[8]
Fructose	H_2O	25	5.5	22.2	71.4	0.5	0.4	Cockman *et al.*[9]

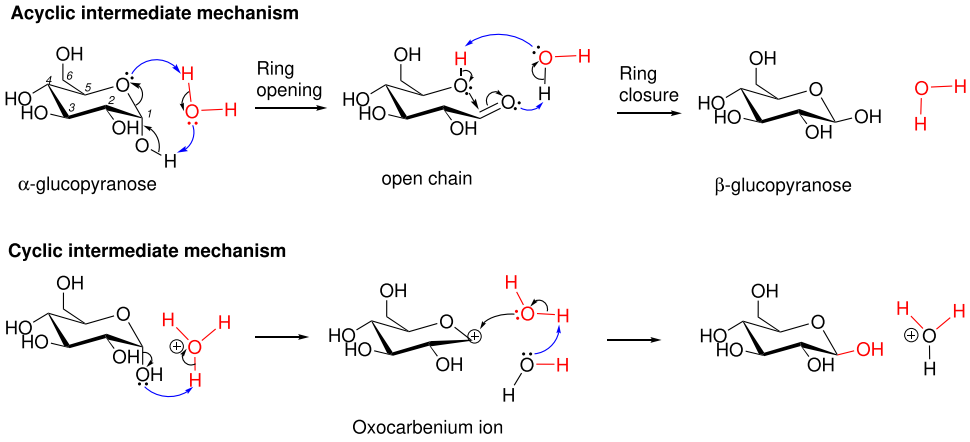

FIG. 2. Glucose mutarotation explained through the acyclic and cyclic intermediate mechanisms. The blue arrows refer to elementary steps of proton transfer. The catalyst (water or the hydronium ion) is depicted in red to highlight the oxygen exchange in the cyclic intermediate mechanism.

the conformational and reactive behavior of carbohydrates has long been recognized, with early *ab initio* molecular dynamics studies already revealing how subtle differences in solvation structure can distinguish the α and β anomers of glucose in water.[20] More recently, computational studies have provided valuable insights into the conformational equilibria of sugars in solution,[21,22] including the calculation of free energy landscapes and mechanisms with enhanced sampling methods.[11,23] A recent experimental study conducted by Trespi and Mazzotti[7] measured the mutarotation rate of lactose in pure water and several mixed aqueous–organic solvents, modeling it as a first-order reversible reaction. The kinetic constant and the activation energy are reported in Table II, together with the values for selected disaccharides and glucose, for comparison. These disaccharides share the commonality that they undergo mutarotation on their glucose residue, exhibiting simple mutarotation similar to that of glucose. Indeed, lactose, the sugar of milk, is a disaccharide consisting of a galactose unit connected with a $\beta(1' \rightarrow 4)$-glycosidic bond to a glucose unit, as shown in Fig. 3. Melibiose, differently from lactose, has a $\beta(1' \rightarrow 6)$-glycosidic bond. Maltose, cellobiose, and gentiobiose consist of two glucose units connected by a $\alpha(1' \rightarrow 4)$-, $\beta(1' \rightarrow 4)$-, or $\beta(1' \rightarrow 6)$-glycosidic bond, respectively. The data in Table II confirm the similar reaction rate and activation energy between these disaccharides and glucose.

TABLE II. Forward kinetic constant $\alpha \rightarrow \beta$ at 25 °C in water and activation energy of glucose and selected disaccharides undergoing simple pyranose–pyranose interconversion. Since experiments usually report the sum of the forward and backward kinetic constants, a ratio of 1.6 is assumed[7] to compute the forward kinetic constant. Activation energy of 69 kJ mol^{-1} is assumed for gentibiose and melibiose to correct the experimental results from 20 to 25 °C.

Sugar	k_α (h^{-1})	E_a (kJ mol^{-1})	Source
Glucose	0.88	NA	Libnau *et al.*[24]
	0.84	68.1	Ballash and Robertson[12]
	0.78	NA	Pazourek[25]
	1.06	63.1	Srisa-nga and Flood[26]
Lactose	0.68	72.7	Trespi and Mazzotti[7]
	0.66	NA	Capon[13]
Melibiose	1.2	NA	Capon[13]
Maltose	0.75	NA	Capon[13]
	0.88	74.4	Srisa-nga and Flood[26]
Cellobiose	0.78	58.5	Srisa-nga and Flood[26]
Gentiobiose	1.16	NA	Capon[13]

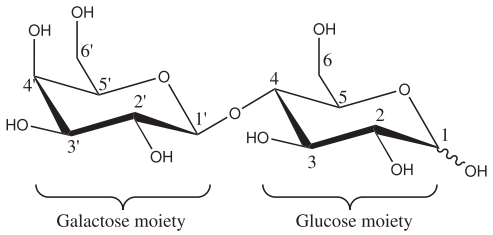

FIG. 3. Lactose molecule, consisting of a galactose and a glucose moiety, and conventional numbering of carbon atoms. The wavy C_1–OH bond indicates that the hydroxyl group can be either axial (α-lactose) or equatorial (β-lactose).

In addition, experimental evidence suggests that the composition of the solution significantly affects the kinetics of mutarotation. Trespi and Mazzotti[7] demonstrated that organic co-solvents in aqueous solution reduce the rate of mutarotation. This effect appears to be directly related to the availability of water molecules participating in the reaction mechanism, as it persists even in mixtures of water and N-methylformamide, which has a higher dielectric constant than pure water, thus ruling out non-specific electrostatic screening as the primary cause. Furthermore, the observation that, at a fixed molar fraction of organic solvent, alcohols yield higher mutarotation rates than aprotic solvents such as DMSO or acetone suggests a key role for hydrogen-bond donor moieties. Despite this emerging experimental evidence, molecular-level insights into the reaction mechanism remain limited.

To address this gap while incorporating the experimentally observed solvent effects, it is essential to retain an explicit

description of the solvent environment in computational studies. Here, we combine well-tempered metadynamics (WTmetaD),[27] mean force integration (MFI),[28,29] and transition state theory (TST)[30–32] to elucidate the solvent-mediated mechanism and kinetics of glucose mutarotation in both aqueous and mixed-solvent systems. In particular, we aim to (i) characterize with atomistic resolution the elementary steps of the mutarotation mechanism in explicit solvent, (ii) quantify the effect of solvent composition on reaction kinetics, and (iii) compare rate estimates with mutarotation experiments obtained from experimental measurements.

II. METHODS

A. Simulation details

A cubic box containing one glucose molecule and six water molecules is first equilibrated in a constant pressure ensemble (NPT) using the Nosé–Hoover barostat.[33,34] The same setup is used for simulations with organic solvents, except that one molecule of methanol and acetone is added, respectively. The system is modeled with the GFN1 xTB semi-empirical method.[35] After equilibrating volume and temperature, the system undergoes 500 ps production metadynamics runs. The average equilibrium volume in the temperature range between 410 and 710 K is 0.343 nm^3. Throughout all the equilibration and metadynamics simulations, we have adopted a time step of 0.5 femtoseconds (fs) and a thermostat relaxation time of 50 fs.

B. Sampling strategy

The sampling of reactive events is enhanced with well-tempered metadynamics (WTmetaD). This technique introduces a time-dependent repulsive bias potential as a function of a low-dimensional set of collective variables (CVs). CVs are a function of the atomic coordinates and approximate the reaction coordinate associated with the studied rare event of interest. In this paper, we selected different *bias factor* (γ) values for various temperatures, namely, $\gamma = 7$ at 710 K and $\gamma = 9$ at 410 K. The initial height of the bias potentials w_0 has been set to 15 kJ/mol in all cases. The width of the WTmetaD Gaussians was determined by unbiased fluctuations of the respective CVs and is discussed in the following.

The elevated simulation temperatures (410–710 K) ensure an efficient exploration of reactive pathways compared to ambient temperature conditions, where effective sampling would be impractically inefficient. Notably, the extrapolation of the resulting rate constants via Arrhenius analysis allows for a direct comparison with experiments at room temperature.

The opening and closure of the glucose ring are hypothesized to follow two distinct pathways, with and without solvent participation. As such, we have performed two independent metadynamics campaigns: one for the water-catalyzed ring-opening step and one for the intramolecular ring-closure. This rationalization of the sampling strategy is necessary due to the limited amount of practically accessible samples and the asymmetry of the reaction mechanism. To enhance the sampling of ring opening events, we used two collective variables: CV_1, the distance between the anomeric carbon C_1 and the ring's oxygen O_5 ($d_{C_1-O_5}$ in Fig. 4), and CV_2, the coordination number of oxygen O_5 with any of the hydrogen atoms in the solvent, expressed as in the following equation:

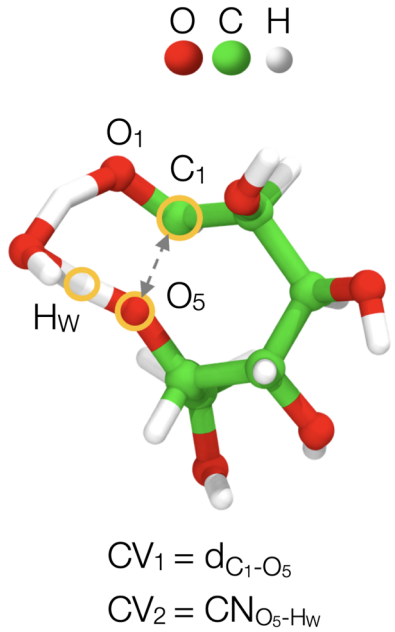

FIG. 4. Definition of the collective variable (CV) space used in metadynamics simulations of the glucose mutarotation reaction. The ring opening reaction is characterized by a two-dimensional CV set: (1) the coordination number $CN_{O_5-H_W}$, which quantifies the degree of hydrogen bonding between the ring oxygen (O_5) of glucose and surrounding water hydrogen atoms (H_W), and (2) the distance $d_{C_1-O_5}$ between the anomeric carbon (C_1) and the ring oxygen (O_5), which serves as a direct measure of the ring opening progress.

$$CN_{O_5H_W} = \sum_{i \in H_W} \frac{1-\left(\frac{r_i-r_0}{r_0}\right)^n}{1-\left(\frac{r_i-r_0}{r_0}\right)^m}, \tag{1}$$

where r_0 is the equilibrium distance of the covalent bond between hydrogen and oxygen, i.e., 1.5 Å. The variable $r_{O_5,i}$ is the distance between the oxygen O_5 and the ith hydrogen atom of the surrounding environment. The exponents m and n are set to 8 and 16, respectively.

The effective reaction coordinate for ring closure simulations is the distance $d_{O_5-C_1}$ only. Normal mode analysis performed using the Gaussian 16 software[36] was used to compute the imaginary frequencies for calculating quantum tunneling corrections. Throughout our simulation campaign, the width of the additive Gaussian terms defining the history-dependent WTmetaD bias potential has been set to 0.05 for CV_1 and 0.02 for CV_2.

C. Free energy surface from multiple independent simulations

The free energy surface in the effective reaction coordinate space defined by the CVs described above is obtained by overlapping multiple independent production runs of 500 ps each. To this end, we have adopted the mean force integration (MFI) algorithm[28] as implemented in the *pyMFI* package.[29] MFI enables the estimation of the free energy surface in CVs space **s** by generalizing the Umbrella Integration (UI) algorithm[37] to time-dependent biases, as

discussed in Refs. 28 and 29. Moreover, it enables the self-consistent combination of samples obtained from independent metadynamics simulations. Within MFI, a free energy surface $F(\mathbf{s})$ is computed by integrating the mean force $\langle \nabla F(\mathbf{s}) \rangle_N$,

$$F(\mathbf{s}) = -\int \mathrm{d}^n \mathbf{s} \langle \nabla F(\mathbf{s}) \rangle_N, \tag{2}$$

where n is the dimensionality of the CV space $\mathbf{s}$ and N is the number of independent simulations merged as

$$\langle \nabla F(\mathbf{s}) \rangle_N = \frac{\sum_{k=1}^{N} W_k \langle \nabla F_{T_k}(\mathbf{s}) \rangle}{\sum_{k=1}^{N} W_k}, \tag{3}$$

where T_k is the total number of bias updates of the kth simulation. The number of independent simulations used in this work is $N = 3$ for each temperature. For each independent simulation, the thermodynamic force in $\mathbf{s}$ at time t, i.e., $\nabla F_t(\mathbf{s})$, is given by

$$\nabla F_t(\mathbf{s}) = -\nabla \beta^{-1} \ln p_t^b(\mathbf{s}) - \nabla V_t(\mathbf{s}), \tag{4}$$

where $p_t^b(\mathbf{s})$ is the probability density of $\mathbf{s}$ under the effect of the bias, $V_t(\mathbf{s})$ is the bias potential at time t, and $\beta = (k_B T)^{-1}$. As in Umbrella Integration, the estimate of the average sampled mean force is given by the weighted average of $\nabla F_t(\mathbf{s})$ with $p_t^b(\mathbf{s})$ acting as weight.

III. RESULTS AND DISCUSSION

A. Water-catalyzed ring opening

The free energy surfaces of ring opening in pure water, in water/methanol, and water/acetone mixtures are reported in Fig. 5. Overall, three distinct equilibrium configurations, local minima on the free energy surface, are found. By following the order of the acyclic intermediate mechanism (Fig. 2), the first is the stable α-glucose pyranose ring, then the configuration related to the protonation of the O_5, and finally, the open chain (acyclic) conformation. These three states represent the sequential reaction steps: the initial cyclic conformation of glucose, a reactive intermediate stabilized through hydrogen bonding with the solvent, and the final linear form resulting from C–O bond cleavage. By comparing the minimum free energy pathways in pure water and water/organic cases, it stands out that the protonated configuration is thermodynamically more stable with respect to the α-glucose pyranose ring when the organic solvents are present. This observation highlights how

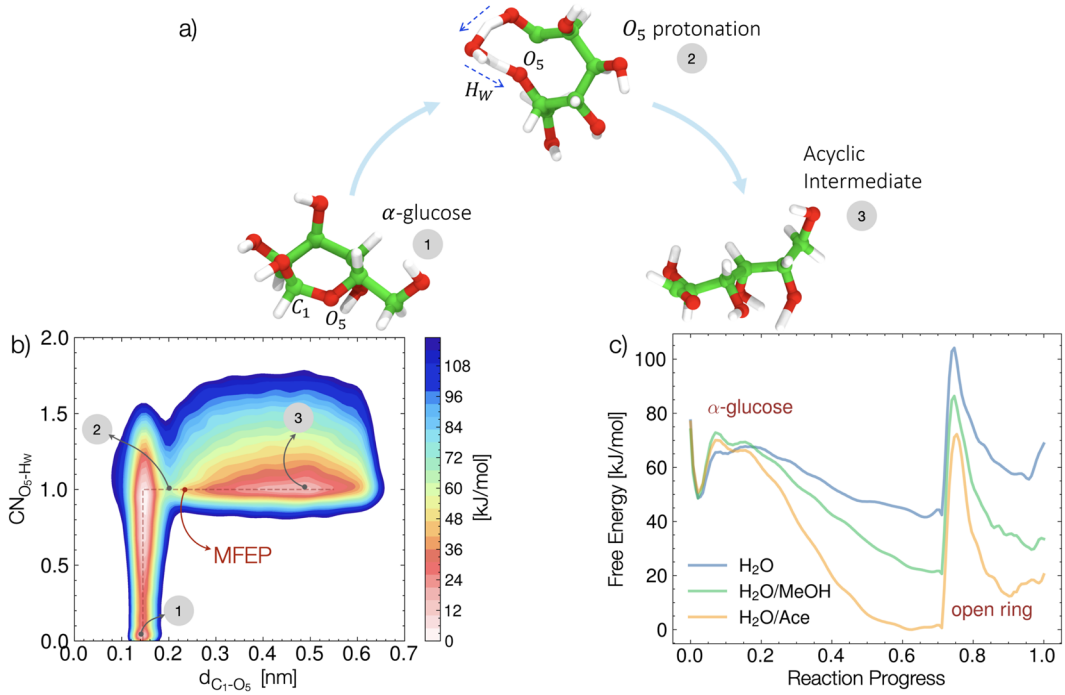

FIG. 5. Free energy landscape and mechanistic representation of the water-catalyzed ring opening of α-glucose at 710 K. (a) Atomistic representations of the key intermediates along the reaction pathway: (1) the reactant α-glucose in its pyranose form; (2) a representative configuration of the ring-opening transition state ensemble in which a hydrogen from a water molecule (H_W) is transferred to the ring oxygen O_5; and (3) the open-chain (acyclic) form of glucose following breakage of the C_1–O_5 bond. The arrows indicate the progression of the mutarotation mechanism via the acyclic intermediate pathway. (b) Two-dimensional free energy surface (FES) as a function of the distance $d_{C1\text{–}O5}$ and the coordination number CN_{O5-H_W}, capturing the hydrogen bond dynamics between O_5 and solvent hydrogen atoms. The minimum energy pathway (MFEP), shown in red, connects the three main basins corresponding to the α-glucose ring, a protonated α-glucose intermediate, and the open-chain conformation. (c) One-dimensional projections of the free energy profiles along the ring-opening reaction coordinate for three solvent systems: pure water (blue), water/methanol (green), and water/acetone (orange). All three systems exhibit the same sequence of states—α-glucose, O_5-protonated intermediate, and open-chain form (3)—but differ significantly in the thermodynamic stabilization of the protonated intermediate, and the free energy barrier associated with the C–O covalent bond breaking.

subtle changes in the solvent environment can substantially modulate the relative energetics of the intermediates, thereby altering the shape and height of the free energy barriers. We justify this result by considering that the presence of organic molecules disrupts the solvation pattern of α-glucose in water, thus altering the relative stability of the intermediates involved in the protonation mechanism of O_5.

The first effect observed is that the barrier associated with the first reactive step, connecting intermediates 1 and 2 in Fig. 5(a), likely arises from the competitive coordination of glucose by the organic co-solvent, which affects the availability and organization of water molecules critical for the concerted proton transfer mechanism.

Instead, the stabilization of the protonated intermediate is likely amplified by the small size of the systems investigated here, where the presence of co-solvents is modeled by adding one molecule in a small solvation shell containing six water molecules. In such a confined environment, each added solvent molecule exerts a disproportionately large influence on the hydrogen-bonding network and local polarity. Consequently, even a single co-solvent molecule can significantly perturb the energetics of the proton transfer step, leading to a differential stabilization of the intermediate state across solvent compositions. Moreover, a qualitative study of the reactive trajectories obtained with WTmetaD showed that the protonation mechanism can occur with concerted participation of one, two, or, less likely, three water molecules. The free energy landscapes reported in Fig. 5 are obtained by selecting only trajectories involving the participation of one water molecule, as this is the most representative pathway observed in the simulation.

The final step, yielding the acyclic intermediate labeled (3) in Fig. 5, requires breaking the covalent bond between the anomeric carbon C_1 and the ring's oxygen O_5, and has an activation free energy markedly dependent on the solution environment. This bond cleavage represents the decisive transformation from the cyclic to the linear form, completing the ring-opening process that underpins mutarotation. For instance, at 710 K, the free energy barrier associated with this second step is 64 kJ/mol in pure water, 68 kJ/mol in the water/methanol mixture, and 72.5 kJ/mol in the water/acetone mixture. The GFN1-xTB is not specifically parameterized for predicting barrier heights of chemical reactions; nevertheless, the work of Bannwarth *et al.*,[38] it shows MADs within 8–38 kJ/mol for the GMTKN55 dataset, which encompasses a wide range of activation barriers and transition state energies. Nonetheless, the method allows for assessing qualitatively the relative impact of organic co-solvents on the activation free energy barriers. The observed increase in activation barrier upon introducing organic co-solvents reflects a clear energetic penalty associated with ring opening in less polar or more structurally disruptive solvent environments. This also clearly indicates a marked dependence of the overall isomerization process on the environment, with lower isomerization kinetics in the presence of organic solvents. From a mechanistic standpoint, this can be attributed to the co-solvents' interference with the hydrogen bonding network and their effect on stabilizing the transition state, which involves a partially broken C–O bond and rearranged solvation shell. In particular, aprotic solvents such as acetone may be less capable of stabilizing charged or polar transition states through hydrogen bonding, thereby raising the activation free energy (see Figs. S1 and S2 of the supplementary material). Remarkably, this observation is consistent with experimental measurements in different solvents,[7] which report a significant reduction in the mutarotation rate of lactose with increasing organic solvent content.

B. Ring closure

Sampling the ring closure has been carried out starting from the open-chain aldehyde configuration, which is characterized by a broad configurational space, and selecting the metadynamics trajectories that lead to the closed ring in the β configuration. We have found that the ring closure can occur with the participation of water in a concerted manner, as depicted in Fig. 6. Our simulations reveal that the presence of water can also facilitate the transformation from the open-chain aldehyde to the cyclic β-anomer. In WTmetaD simulations, where the sole CV_1 is biased, we observed how a water molecule mediates a synchronized proton transfer by accepting a proton from the hydroxyl group on O_5, facilitating its nucleophilic attack on the anomeric carbon C_1, while simultaneously donating a proton to the aldehyde oxygen. The resulting 50 kJ/mol free energy barrier at 710 K confirms that the ring closure is kinetically less demanding than the ring-opening step.

C. Mutarotation kinetics

Based on the results gathered from enhanced sampling, we can identify the ring-opening step connecting the protonated and the acyclic intermediates as the rate-determining step of the mutarotation reaction. The kinetic rate parameters of the ring opening

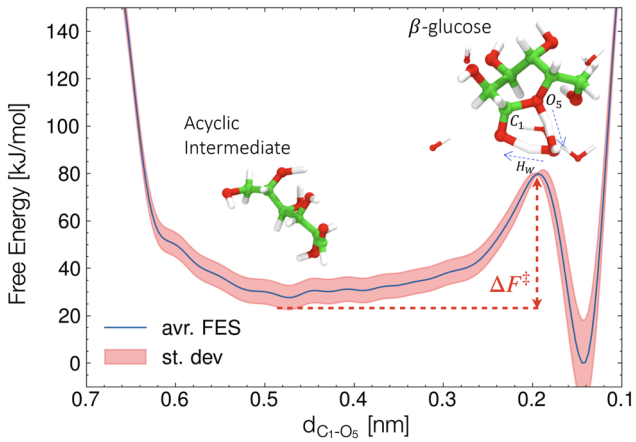

FIG. 6. Free energy profile for the ring closure step from the acyclic intermediate to β-glucose in aqueous solution. One-dimensional free energy surface (FES) as a function of the distance $d_{C1\text{–}O5}$, representing the formation of the C_1–O_5 bond that completes the isomerization of α-glucose. The blue line corresponds to the average FES computed from three independent well-tempered metadynamics simulations, and the shaded pink region indicates the associated standard deviation. The acyclic intermediate corresponds to large $d_{C1\text{–}O5}$ values, while the β-glucose cyclic product lies at short distances. The transition state, located at ~0.21 nm, is associated with an activation free energy barrier $\Delta F^{\ddagger}$ of ≈50 kJ/mol at 710 K. The structural snapshots illustrate the start and end points of the ring closure process: the open-chain conformation and the final β-anomeric pyranose form. Notably, a water molecule (H_W) participates in the transformation by mediating a concerted proton transfer between the ring oxygen (O_5) and the aldehyde oxygen at C_1, facilitating bond formation.

reaction are calculated using the canonical transition state theory formulation, including the tunneling correction and the presence of the O_5-protonated intermediate uncovered via sampling,

$$k_{\text{opening}} = \frac{k_B T}{h} Q_{tunn} \frac{Q^I}{Q^R} e^{-\frac{\Delta F^{\ddagger}_{ro}}{k_B T}}, \tag{5}$$

where Q^I and Q_R are the canonical partition functions of the protonated intermediate and reactant, respectively, while $\Delta F^{\ddagger}_{ro}$ is the activation free energy of the ring-opening step identified as the rate determining step shown in Fig. 7(a). The tunneling correction is required since the protonation of O_5 involves the transfer of a hydrogen atom. The impact of tunneling corrections to the accuracy of hydrogen transfer reactions has been extensively discussed in the literature.[39–41]

The ratio between canonical partition functions is calculated by integrating the Boltzmann factor along the minimum free energy pathway as

$$\frac{Q^I}{Q^R} = \frac{\int_{\Omega_I} e^{-\beta F(s)} ds}{\int_{\Omega_R} e^{-\beta F(s)} ds}. \tag{6}$$

The integral in the numerator is performed over Ω_I, which represents the ensemble of O_5-protonated configurations, identified as a stable intermediate state preceding the ring opening step. To this end, we considered the minimum free energy profile along the coordination number $CN_{O_5-H_W}$ by fixing the distance $d_{C_1-O_5}$ corresponding to the closed ring. We then considered Ω_I as the interval of coordination numbers determined by the amplitude of a quantum harmonic oscillator centered in the O_5-protonated intermediate, where $CN_{O_5-H_w} = 0.947$. The amplitude of the quantum harmonic oscillator is calculated with the following, well-known, relation:

$$A^{\max} = \sqrt{\frac{2U_{vib}}{\mu\omega^2}}, \tag{7}$$

where μ is the reduced mass of the O_5–H_W bond and ω is the pulsation of the harmonic oscillator calculated as $2\pi\nu$. The internal energy of the quantum harmonic oscillator U_{vib} is calculated as in

$$U_{vib} = h\nu N_{av}\left(\frac{1}{2} + \frac{e^{-\beta h\nu}}{1 - e^{-\beta h\nu}}\right), \tag{8}$$

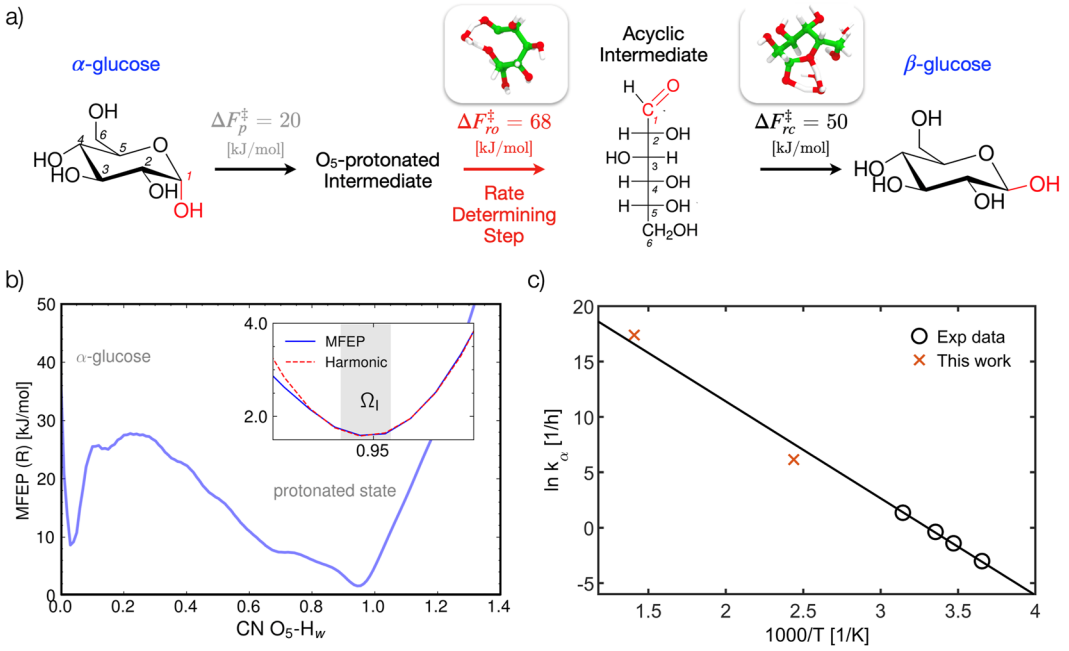

FIG. 7. Kinetic analysis of glucose mutarotation via the acyclic intermediate mechanism. (a) Reaction scheme for glucose mutarotation via the acyclic intermediate mechanism, as revealed by enhanced sampling simulations. The pathway proceeds through four key intermediates- α-glucose, O_5-protonated α-glucose, and the acyclic open-chain form-before ring closure yields β-glucose. The free energy barriers for each elementary step are extracted from the computed free energy surface (710 K, pure water) for the protonation step ($\Delta F^{\ddagger}_{p}$), ring opening ($\Delta F^{\ddagger}_{ro}$), and ($\Delta F^{\ddagger}_{rc}$). The molecular structures depict the transition states identified between these intermediates and illustrate the emergence of a unifying mechanistic feature: in all cases, hydrogen-bond donor solvent molecules play a critical role in stabilizing the transition state. Ring opening is identified as the rate-determining step. (b) Free energy profile associated with the metastable O_5-protonated free energy minimum. The shaded region defines the ensemble of protonated configurations (Ω_1) used to compute the partition function for the intermediate state used in the rate expression. The inset compares the MFEP with a harmonic approximation around the protonated minimum. (c) Arrhenius plot of the $\alpha \rightarrow \beta$ mutarotation rate constant (k_α) as a function of inverse temperature. Orange crosses represent the values computed in this work from metadynamics simulations combined with transition state theory and tunneling corrections. Extrapolation of the experimental data on lactose mutarotation from Trespi and Mazzotti[7] agrees well with the predicted kinetic constants of this work.

where h is the Planck constant and N_{av} is the Avogadro number. Finally, the value of ν has been computed through frequency analysis using the GGA DFT method, ωB97XD/def2TZVPP. By averaging the frequencies of the modes that impact the O_5–H_W bond, we found an average frequency of 450 cm^{-1}. This corresponds to an internal energy of 6.3 kJ/mol and defines an interval of coordination numbers of width 0.05 [shown in the inset of Fig. 7(b) with a gray-shaded area]. The imaginary frequency found for the transition state with one water molecule, corresponding to the FES reported in Fig. 5, is 1140 cm^{-1}. In addition, it is worth mentioning that the free energy profile could be accurately determined by fitting the free energy well associated with the protonated state with a quadratic function, as shown in Fig. 7(b).

We account for tunneling effects using the Eckart tunneling partition function, which is determined by the forward and backward barriers associated with the protonation of the α anomer, as identified in the minimum free energy pathway and the imaginary frequency. At 710 K, the Eckart tunneling correction is 1.2, whereas at 410 K, it is 1.86. We have performed simulations at a higher temperature with respect to the experiments to achieve a faster sampling of the reaction free energy landscape. Nevertheless, in Fig. 7 we compared our predicted ring-opening kinetic constants of glucose with the forward mutarotation kinetic constants extrapolated from the work of Trespi and Mazzotti[7] on lactose mutarotation. The agreement supports the hypotheses that (i) the reactivities of lactose and glucose are similar and that (ii) ring-opening is the actual rate-determining step of mutarotation, i.e., $k_\alpha \sim k_{\text{opening}}$. Moreover, the agreement between the Arrhenius extrapolation of the experimental data under ambient conditions and the computed rate constants at high T [Fig. 7(c)] further validates the sampling strategy followed to compute free energy profiles.

IV. CONCLUSIONS

The water-catalyzed mechanism of lactose mutarotation has been investigated through well-tempered metadynamics in pure water and water–organic mixtures. Motivated by experimental observations of reduced $\alpha \rightarrow \beta$ mutarotation rates in the presence of organic co-solvents, we conducted simulations in water/methanol and water/acetone mixtures. Given that mutarotation occurs on the glucose moiety of the lactose molecule, glucose was adopted as a chemically faithful and computationally tractable model system. The mechanism was explored via two sets of independent WTmetaD simulations: one for the water-catalyzed ring-opening step and one for the ring closure into the β-anomer configuration. The free energy landscapes obtained at 410 and 710 K confirm that ring opening is the rate-determining step, in agreement with previous studies.[11,12] Crucially, finite-temperature sampling of reactive trajectories reveals that both ring opening and ring closure proceed via solvent-assisted, concerted mechanisms, involving one or more water molecules in the transition state. This underscores the central catalytic role of the solvent, which emerges spontaneously without being enforced by the simulation setup.

These findings extend early *ab initio* simulations of glucose in water by Molteni and Parrinello,[20] which first demonstrated anomer-dependent solvation structures by showing how the solvent not only differentiates anomer stability but also actively mediates reactivity along the mutarotation pathway. Furthermore, the rate estimates obtained from our simulations are in good agreement with experimental measurements by Trespi and Mazzotti,[7] implying that the underlying mechanistic interpretation captured by our finite-temperature, explicitly solvated simulations is consistent with observed macroscopic kinetics. In this work, we outline a methodology for determining kinetic rate coefficients from well-tempered metadynamics simulations in explicitly solvated systems. The approach yields kinetic parameters and mechanistic insight, capturing how solvent structure and composition reshape the reaction free energy landscape.

We anticipate that combining the methodology outlined here with ML-based interatomic potentials trained on high-quality DFT calculations will broaden their applicability and strengthen the predictive link between molecular simulations and experimentally observed carbohydrate reactivity, enabling a quantitative exploration of the composition dependence of mutarotation kinetics.

SUPPLEMENTARY MATERIAL

The supplementary material encompasses Figs. S1 and S2, displaying the molecular arrangement of the co-solvent molecules around the glucose moiety during the ring-opening process.

ACKNOWLEDGMENTS

The authors acknowledge the CINECA Award No. HP10B98SC8 under the ISCRA initiative for the availability of high-performance computing resources and support. M.S. and M.P. acknowledge funding from the ht-MATTER UKRI Frontier Research Guarantee (Grant No. EP/X033139/1). This study was a contribution to the *Michele Parrinello Festschrift* of *The Journal of Chemical Physics*. We would like to underline how strongly developments in molecular simulations like this one have profited from the pioneering work conducted and from the plethora of more recent theories and tools developed during his extraordinary scientific career by Michele Parrinello. In dedicating this work to him, we would like to draw from the experience of the two senior authors, who have been fortunate enough to have Michele Parrinello as mentor, collaborator, and friend, to underline how stimulating, fulfilling, and exhilarating working with him is. His enthusiasm for research and his joy in tackling (and often overcoming) scientific challenges have been hugely inspiring.

AUTHOR DECLARATIONS

Conflict of Interest

The authors have no conflicts to disclose.

Author Contributions

F.S. and S.T. contributed equally to this work.

Francesco Serse: Conceptualization (lead); Investigation (equal); Software (equal); Writing – original draft (equal); Writing – review & editing (equal). **Silvio Trespi**: Conceptualization (lead);

Investigation (equal); Writing – original draft (equal); Writing – review & editing (equal). **Matteo Paloni**: Investigation (supporting); Methodology (supporting); Software (supporting); Supervision (supporting); Writing – review & editing (equal). **Matteo Salvalaglio**: Conceptualization (equal); Funding acquisition (equal); Investigation (equal); Methodology (equal); Supervision (equal); Writing – original draft (equal); Writing – review & editing (equal). **Marco Mazzotti**: Conceptualization (equal); Funding acquisition (equal); Investigation (equal); Supervision (equal); Writing – review & editing (equal).

DATA AVAILABILITY

The data that support the findings of this study are available from the corresponding author upon reasonable request.

REFERENCES

[1] B. D. Smith, "Simplified calculation of chemical equilibria in hydrocarbon systems containing isomers," AIChE J. **5**(1), 26–28 (1959).
[2] R. A. Alberty, "Chemical thermodynamic properties of isomer groups," Ind. Eng. Chem. Fundam. **22**(3), 318–321 (1983).
[3] S. K. Chandrasekaran and C. Judson King, "Solid-liquid phase equilibria in multicomponent aqueous sugar solutions," J. Food Sci. **36**(4), 699–704 (1971).
[4] S. Trespi, S. Roshanfekr, and M. Mazzotti, "Thermodynamics of isomers and solubility prediction in multicomponent sugar solutions," J. Phys. Chem. B **129**(14), 3661–3669 (2025).
[5] C. Vega, H. D. Goff, and Y. H. Roos, "Spray drying of high-sucrose dairy emulsions: Feasibility and physicochemical properties," J. Food Sci. **70**(3), E244–E251 (2006).
[6] J. R. Bourne, M. Hegglin, and J. E. Prenosil, "Solubility and selective crystallization of lactose from solutions of its hydrolysis products glucose and galactose," Biotechnol. Bioeng. **25**(6), 1625–1639 (1983).
[7] S. Trespi and M. Mazzotti, "Kinetics and thermodynamics of lactose mutarotation through chromatography," Ind. Eng. Chem. Res. **63**(12), 5028–5038 (2024).
[8] S. J. Angyal, "The composition of reducing sugars in solution," Adv. Carbohydr. Chem. Biochem. **42**, 15–68 (1984).
[9] M. Cockman, D. G. Kubler, A. S. Oswald, and L. Wilson, "The mutarotation of fructose and the invertase hydrolysis of sucrose," J. Carbohydr. Chem. **6**, 181–201 (1987).
[10] P. Ward and H. S. Isbell, "Mutarotation of sugars in solution: Part I: History, basic kinetics, and composition of sugar solutions," Adv. Carbohydr. Chem. **23**, 11–57 (1968).
[11] H. Cui, R. Lai, S. Yuan, C. Liao, A. Wang, and G. Li, "A reactive force field for molecular dynamics simulations of glucose in aqueous solution," J. Chem. Theory Comput. **19**(13), 4286–4298 (2023).
[12] N. M. Ballash and E. B. Robertson, "The mutarotation of glucose in dimethylsulfoxide and water mixtures," Can. J. Chem. **51**(4), 556–564 (1973).
[13] B. Capon, "Mechanism in carbohydrate chemistry," Chem. Rev. **69**, 407–498 (1969).
[14] D. Rittenberg and C. Graff, "A comparison of the rate of mutarotation and O^{18} exchange of glucose," J. Am. Chem. Soc. **80**, 3370–3372 (1958).
[15] J. M. Risley and R. L. Van Etten, "Kinetics of oxygen exchange at the anomeric carbon atom of D-glucose and D-erythrose using the oxygen-18 isotope effect in carbon-13 nuclear magnetic resonance spectroscopy," Biochemistry **21**, 6360–6365 (1982).
[16] T. L. Mega, S. Cortes, and R. L. Van Etten, "The oxygen-18 isotope shift in carbon-13 nuclear magnetic resonance spectroscopy. 13. Oxygen exchange at the anomeric carbon of D-glucose, D-mannose, and D-fructose," J. Org. Chem. **55**, 522–528 (1990).
[17] B. E. Lewis, N. Choytun, V. L. Schramm, and A. J. Bennet, "Transition states for glucopyranose interconversion," J. Am. Chem. Soc. **128**, 5049–5058 (2006).
[18] I. Alkorta and P. L. A. Popelier, "Computational study of mutarotation in erythrose and threose," Carbohydr. Res. **346**, 2933–2939 (2011).
[19] W. Plazinski, A. Plazinska, and M. Drach, "The water-catalyzed mechanism of the ring-opening reaction of glucose," Phys. Chem. Chem. Phys. **17**, 21622–21629 (2015).
[20] C. Molteni and M. Parrinello, "Glucose in aqueous solution by first principles molecular dynamics," J. Am. Chem. Soc. **120**(9), 2168–2171 (1998).
[21] Q. Liao, M. A. B. Morais, C. Rovira, and A. Nin-Hill, "Conformational free energy landscape of β -glucose in the gas phase and aqueous solution: Energetic, structural, and electronic changes," ACS Omega **10**, 19903 (2025).
[22] K. H. Lee, U. Schnupf, B. G. Sumpter, and S. Irle, "Performance of density-functional tight-binding in comparison to ab initio and first-principles methods for isomer geometries and energies of glucose epimers in vacuo and solution," ACS Omega **3**, 16899–16915 (2018).
[23] D. Liu, M. R. Nimlos, D. K. Johnson, M. E. Himmel, and X. Qian, "Free energy landscape for glucose condensation reactions," J. Phys. Chem. A **114**(49), 12936–12944 (2010).
[24] F. O. Libnau, J. Toft, A. A. Christy, and O. M. Kvalheim, "Structure of liquid water determined from infrared temperature profiling and evolutionary curve resolution," J. Am. Chem. Soc. **116**(18), 8311–8316 (1994).
[25] J. Pazourek, "Monitoring of mutarotation of monosaccharides by hydrophilic interaction chromatography," J. Sep. Sci. **33**(6–7), 974–981 (2010).
[26] S. Srisa-nga and A. E. Flood, "Mutarotation rates and equilibrium of simple carbohydrates," in *Asian Pacific Confederation of Chemical Engineering Congress Program and Abstracts* (The Society of Chemical Engineers, Japan, 2004), pp. 1–10.
[27] A. Barducci, G. Bussi, and M. Parrinello, "Well-tempered metadynamics: A smoothly converging and tunable free-energy method," Phys. Rev. Lett. **100**, 020603 (2008).
[28] V. Marinova and M. Salvalaglio, "Time-independent free energies from metadynamics via mean force integration," J. Chem. Phys. **151**(16), 164115 (2019).
[29] A. Bjola and M. Salvalaglio, "Estimating free-energy surfaces and their convergence from multiple, independent static and history-dependent biased molecular-dynamics simulations with mean force integration," J. Chem. Theory Comput. **20**(13), 5418–5427 (2024).
[30] F. Serse, A. Bjola, M. Salvalaglio, and M. Pelucchi, "Unveiling solvent effects on β-scissions through metadynamics and mean force integration," J. Chem. Theory Comput. **20**(14), 6253–6262 (2024).
[31] F. Serse, M. Salvalaglio, and M. Pelucchi, "First principles assessment of solvent induced cage effects on intramolecular hydrogen transfer in the free radical polymerization of acrylates," Phys. Chem. Chem. Phys. **27**, 5271 (2025).
[32] B. Peters, *Reaction Rate Theory and Rare Events* (Elsevier Science, 2017).
[33] S. Nosé, "A unified formulation of the constant temperature molecular dynamics methods," J. Chem. Phys. **81**(1), 511–519 (1984).
[34] S. Nosé, "A molecular dynamics method for simulations in the canonical ensemble," Mol. Phys. **52**(2), 255–268 (1984).
[35] S. Grimme, C. Bannwarth, and P. Shushkov, "A robust and accurate tight-binding quantum chemical method for structures, vibrational frequencies, and noncovalent interactions of large molecular systems parametrized for all spd-block elements (Z = 1–86)," J. Chem. Theory Comput. **13**(5), 1989–2009 (2017).
[36] M. J. Frisch, G. W. Trucks, H. B. Schlegel, G. E. Scuseria, M. A. Robb, J. R. Cheeseman, G. Scalmani, V. Barone, G. A. Petersson, H. Nakatsuji, X. Li, M. Caricato, A. V. Marenich, J. Bloino, B. G. Janesko, R. Gomperts, B. Mennucci, H. P. Hratchian, J. V. Ortiz, A. F. Izmaylov, J. L. Sonnenberg, D. Williams-Young, F. Ding, F. Lipparini, F. Egidi, J. Goings, B. Peng, A. Petrone, T. Henderson, D. Ranasinghe, V. G. Zakrzewski, J. Gao, N. Rega, G. Zheng, W. Liang, M. Hada, M. Ehara, K. Toyota, R. Fukuda, J. Hasegawa, M. Ishida, T. Nakajima, Y. Honda, O. Kitao, H. Nakai, T. Vreven, K. Throssell, J. A. Montgomery, Jr., J. E. Peralta, F. Ogliaro, M. J. Bearpark, J. J. Heyd, E. N. Brothers, K. N. Kudin, V. N. Staroverov, T. A. Keith, R. Kobayashi, J. Normand, K. Raghavachari, A. P. Rendell, J. C. Burant, S. S. Iyengar, J. Tomasi, M. Cossi, J. M. Millam, M. Klene, C. Adamo,

R. Cammi, J. W. Ochterski, R. L. Martin, K. Morokuma, O. Farkas, J. B. Foresman, and D. J. Fox, *Gaussian 16 Revision C.01*, Gaussian Inc., Wallingford, CT, 2016.

[37]J. Kästner and W. Thiel, "Bridging the gap between thermodynamic integration and umbrella sampling provides a novel analysis method: 'Umbrella integration,'" J. Chem. Phys. **123**(14), 144104 (2005).

[38]C. Bannwarth, S. Ehlert, and S. Grimme, "GFN2-xTB—An accurate and broadly parametrized self-consistent tight-binding quantum chemical method with multipole electrostatics and density-dependent dispersion contributions," J. Chem. Theory Comput. **15**(3), 1652–1671 (2019).

[39]E. Gonzalez-Lavado, J. C. Corchado, Y. V. Suleimanov, W. H. Green, and J. Espinosa-Garcia, "Theoretical kinetics study of the $O(^3P)$ + CH_4/CD_4 hydrogen abstraction reaction: The role of anharmonicity, recrossing effects, and quantum mechanical tunneling," J. Phys. Chem. A **118**(18), 3243–3252 (2014).

[40]T. Lamberts and J. Kac, "Tunneling reaction kinetics for the hydrogen abstraction reaction H + H_2S → H_2 + HS in the interstellar medium," J. Phys. Chem. A **121**(51), 9736–9741 (2017).

[41]J. Kästner, "Theory and simulation of atom tunneling in chemical reactions," WIREs Comput. Mol. Sci. **4**(2), 158–168 (2014).